Planetary Nebulae Beyond the Milky Way – Historical Overview

Michael J. Barlow

Department of Physics & Astronomy,
University College London,
Gower Street, London WC1E 6BT, U.K.

1 Introduction

Up to 10% of the total luminosity of a planetary nebula, $\sim$500 $L_{\odot}$, can be emitted in the dominant cooling line, [O III] λ5007. This, coupled with the narrowness of the line ($\sim$15-25 km s^{-1}), makes it extremely easy to detect PNe in external galaxies using a narrow-band filter tuned to the galaxy redshift. The availability of multiple independent distance indicators for our closest neighbouring galaxies, the Magellanic Clouds and M 31, means that the luminosities of the PNe in these galaxies (in particular the large numbers of PNe in the LMC) can be used to calibrate PN luminosity functions, which have been used over the past 15 years as probes of the Hubble constant. Given the fact that we still do not have accurate distances for most planetary nebulae in the Milky Way, this has been an astonishing development. Unlike H II regions, which cannot be used to probe elliptical galaxies, planetary nebulae can be used to probe the dynamics and metallicity of any type of galaxy. Today, via accurate radial velocity measurements, extragalactic PNe are being used as dynamical mass probes of galaxies, and even of the stellar mass content of the intracluster regions of galaxy clusters, with dedicated 'planetary nebula spectrographs' being built to further such studies. The angular resolution of the Hubble Space Telescope has turned out to be ideally suited to the study of PNe in the LMC and SMC, and the exploitation of the accurately known distances to these two galaxies has allowed reliable luminosities and masses to be derived for the central stars and nebulae, thereby putting PN research on a much more quantitative footing.

In this overview of past and recent studies of extragalactic planetary nebulae (PNe), I have divided the research into two main areas: (a) surveys for planetary nebulae in other galaxies, PN luminosity functions and intracluster PNe; (b) detailed studies of planetary nebulae in the Magellanic Clouds, particularly studies carried out with the HST.

2 Surveys for Extragalactic Planetary Nebulae

The low dust extinctions to the LMC and SMC mean that virtually all nebulae present can be detected by a survey down to a given intrinsic luminosity limit. The low reddening also makes them well suited to study in the ultraviolet. Sanduleak, MacConnell & Philip (1978: SMP) published a catalogue of all PNe

M.J. Barlow, Planetary Nebulae Beyond the Milky Way – Historical Overview. In: Planetary Nebulae Beyond the Milky Way, L. Stanghellini et al. (eds.), ESO Astrophysics Symposia, pp. 3–14 (2006)
DOI 10.1007/11604792_1

that had been discovered in the Magellanic Clouds up till then. Of the 28 SMC PNe in their list, 18 had been discovered by Henize (1956), 7 were from Lindsay (1961) and 3 came from SMP's own objective prism survey. Of the 102 LMC PNe in their list, 59 were from Henize (1956), 21 came from Lindsay & Mullan (1963) and 22 came from their own objective prism survey.

Ford et al. (1973) detected 26 PNe in the dwarf elliptical companion galaxies to M 31: NGC 185, NGC 205 and NGC 221, via filter imaging in [O III] and Hα. Ford & Jenner (1975) followed up with deeper observations of NGC 221, detecting 21 PNe in its field (see Fig. 1). Three of the 14 PNe with observed radial velocities belonged to M 31, the rest to NGC 221 (they were distinguished by means of the 200 km s^{-1} difference between the two galaxies).

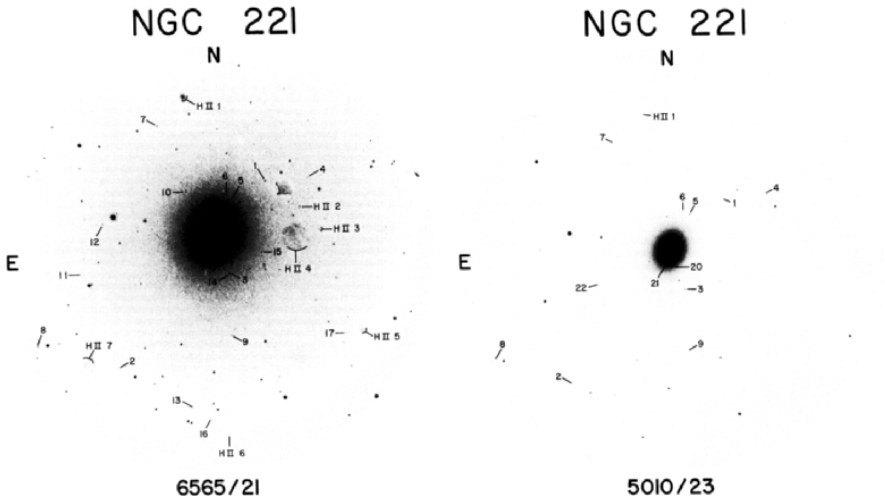

Fig. 1. Hα (left) and [O III] (right) images of NGC 221 (= M 32). The central wavelengths and widths (in Å) of the filters are indicated at the bottom of the figures. From Ford & Jenner (1975).

A deep narrow-band [O III] and Hα filter survey by Jacoby (1980) led to the detection of 53 faint new SMC and LMC PNe in selected fields and the derivation of a PN luminosity function (PNLF) that reached six magnitudes below the brightest. This work led the foundations for subsequent studies that exploited PNLF's for more distant galaxies. Ciardullo et al. (1989a) detected 429 PNe in the bulge of M 31, of which 104 were in the first 2.5 mags of its PNLF (Fig. 2). A steep turnover observed at the high luminosity end was interpreted as corresponding to a sharp cutoff in the upper mass limit of PN central stars, consistent with the expectation that no central star should exceed the Chandrasekhar mass limit and that they should evolve increasingly quickly as this mass is approached.

Ciardullo, Jacoby & Ford (1989b) detected 249 PNe in three early type galaxies in the Leo I cluster: NGC 3377 (E6), NGC 3379 (E0) and NGC 3384 (S0).

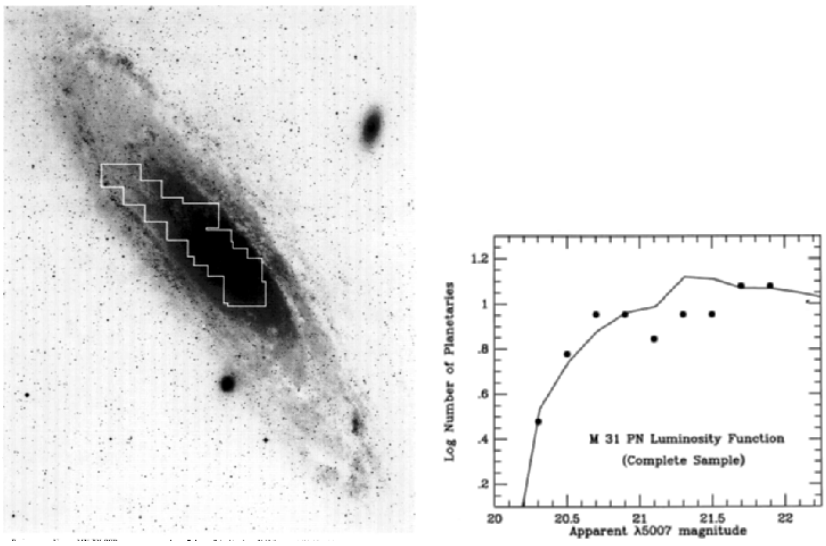

Fig. 2. Image of M 31 (left), showing the region surveyed for PNe using an [O III] 5007 Å filter. The plot on the right shows the resulting PN luminosity function for the 429 PNe discovered, from Ciardullo et al. (1989a)

All had similar PN [O III] luminosity functions, indistinguishable from those observed in the spiral galaxies M 31 and M 81. The PNLF invariance with galaxy type and metallicity demonstrated the PNLF to be an excellent standard candle. Model simulations indicated a central star mass distribution highly peaked at $\sim$0.6 M$\odot$, similar to that of nearby white dwarfs.

PNe are now routinely used to study the internal dynamics and mass distributions of both early and late type galaxies, e.g. Arnaboldi et al. (1998) have measured the rotation curve and velocity dispersions along two axes of the early type galaxy NGC 1316 (Fornax A) from radial velocity measurements of 43 PNe (Fig. 4). The total galaxy mass inside 16 kpc radius was derived to be 2.9×10^{11} solar masses.

Méndez et al. (2001) detected 535 PNe in the elliptical galaxy NGC 4697 using filter images and slitless spectra. The former gave the [O III] PNLF (Fig. 3, right), which yielded a distance of 10.5 Mpc. The latter gave radial velocities for 531 of the PNe, allowing an accurate mass to luminosity ratio to be derived for the galaxy.

Turning to more local regions, Magrini et al. (2003) have surveyed a number of Local Group dwarf galaxies for PNe. They found that the number of PN per unit stellar luminosity appears to decline steeply for metallicities below 0.1 solar (Fig. 5).

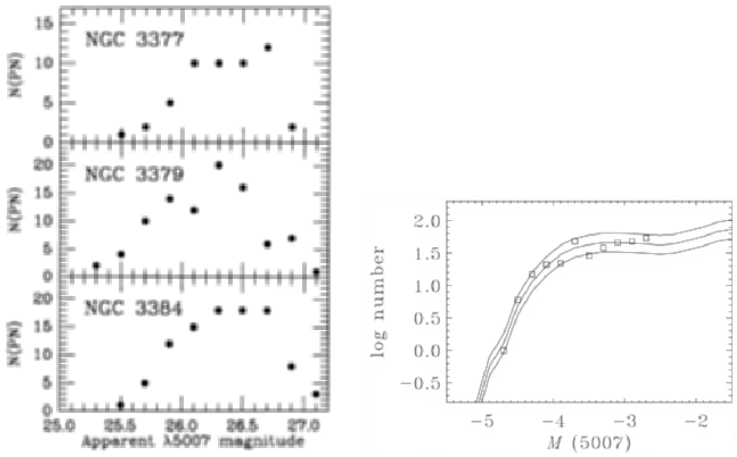

Fig. 3. [O III] PNLF's for three Leo I galaxies (left), derived by Ciardullo et al. (1989b). The plot on the right shows the [O III] PNLF derived by Méndez et al. (2001) for 535 PNe in the elliptical galaxy NGC 4697, which is located in the Virgo southern extension. The three lines show PNLF simulations from Méndez & Soffner (1997), for three different sample sizes: 2500, 3500, and 4900 PNe.

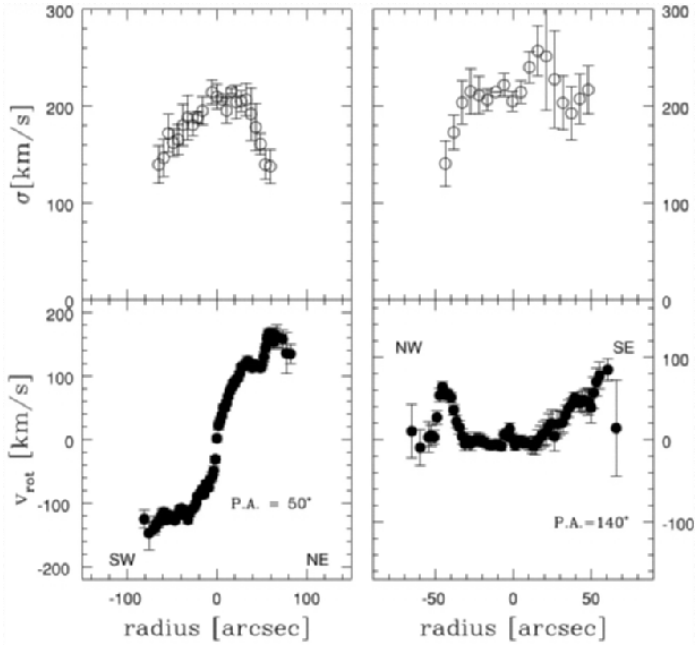

Fig. 4. Velocity dispersions (upper) and rotation curves (lower) for NGC 1316. From Arnaboldi et al. (1998).

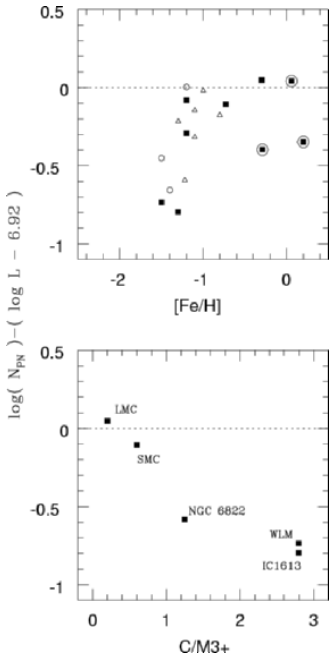

Fig. 5. Number of planetary nebulae per unit galactic luminosity as a function of galaxy metallicity (upper) and as a function of the ratio of carbon stars to O-rich late-type AGB stars (lower). From Magrini et al. (2003).

3 Planetary Nebulae in the Intracluster Regions of Galaxy Clusters

Arnaboldi et al. (1996) measured radial velocities for 19 PNe in the outer regions of the giant elliptical galaxy NGC 4406, in the southern Virgo extension region. Although this galaxy has a radial velocity of –227 km s^{-1}, three of the PNe had radial velocities close to 1400 km s^{-1}, the mean radial velocity of the Virgo cluster. It was concluded that they were intracluster PNe. Theuns & Warren (1997) discovered ten PN candidates in the Fornax cluster, in fields well away from any Fornax galaxy – consistent with tidal stripping of cluster galaxies. They estimated that intracluster stars could account for up to 40% of all the stars in the Fornax cluster.

Méndez et al. (1997) surveyed a 50 $arcmin^2$ area near the centre of the Virgo cluster, detecting 11 PN candidates. They estimated that a stellar population comprising $4{\times}10^9$ $M_\odot$ lay in their survey area and that such a population could account for up to 50% of the total stellar mass in the Virgo cluster. Feldmeier, Ciardullo & Jacoby (1998) searched for intracluster PNe in several Virgo Cluster fields. Comparison with the normalised M 87 PNLF showed an excess at the bright end, attributed by them to intracluster PNe (see Fig. 6).

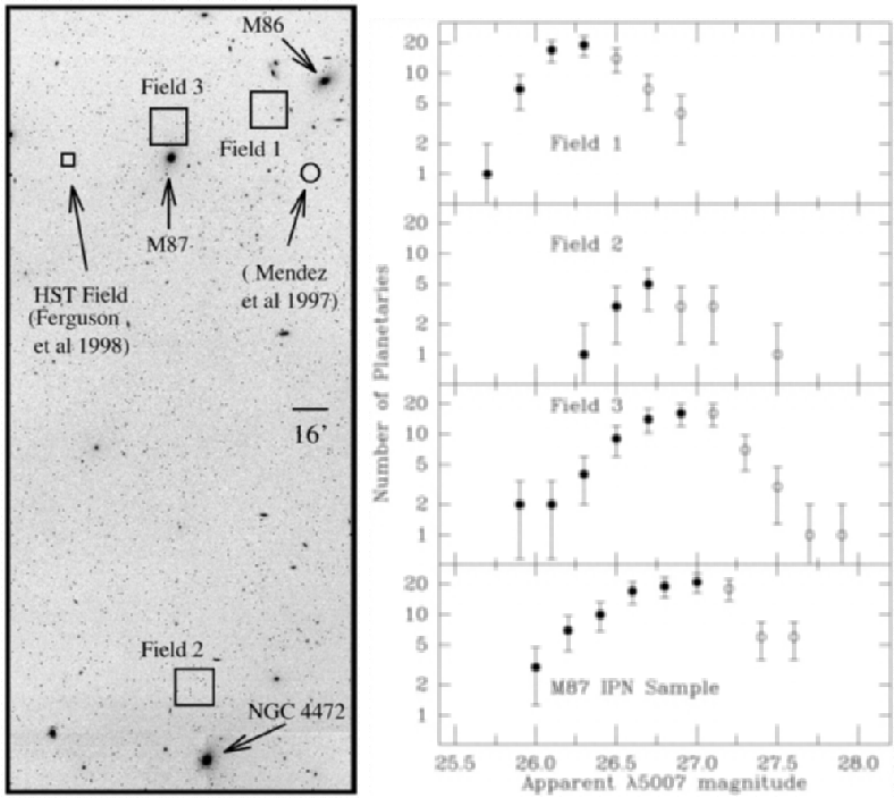

Fig. 6. Left: Virgo cluster fields searched for PNe by Feldmeier et al. (1998). Right: the resulting PN luminosity functions.

4 Observations of Magellanic Cloud Planetary Nebulae

Magellanic Cloud PNe are bright enough that Dopita et al. (1988) were able to obtain echelle spectra with 11.5 km s $^{-1}$ resolution of 94 LMC PNe in the [O III] 5007 Å line, using 1.0 m and 2.3 m telescopes. The nebulae were spatially unresolved from the ground but those with asymmetric velocity profiles (Fig. 7) indicate non-spherically symmetric nebulae. The radial velocities were used by Meatheringham et al. (1988) to conduct a dynamical study of the PN population in the LMC.

Monk et al. (1988) analysed 3.9-m AAT spectra of 21 SMC and 50 LMC PNe. They found that the PN and H II region abundances of oxygen and neon agreed within the same galaxy but that nitrogen in the planetary nebulae was enhanced by 0.9 dex in both the SMC and LMC. This was interpreted by them as due to CN cycle processing of almost all of the original carbon into nitrogen at the time of the first dredge-up. This process appears to have operated much

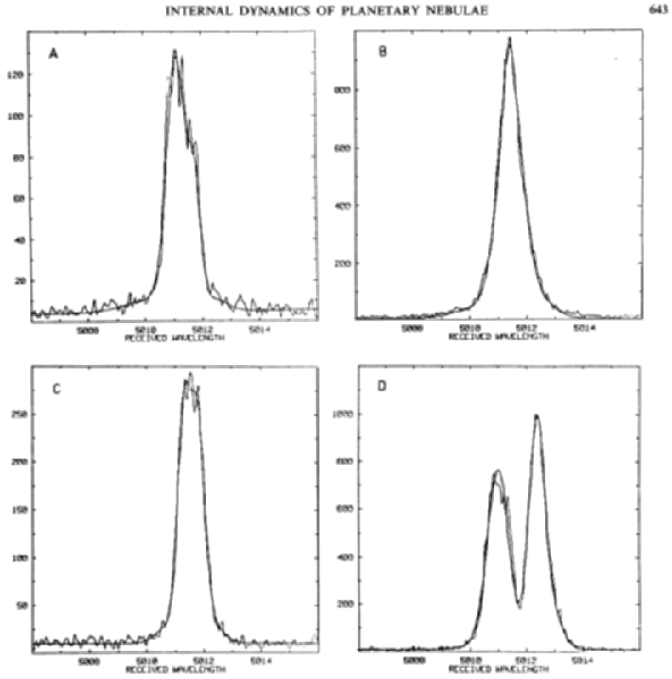

Fig. 7. High spectra resolution profiles of the [O III] 5007 Å line for four LMC PNe. Asymmetric or double-peaked profiles indicate non-spherically symmetric nebulae. From Dopita et al. (1988).

more efficiently in the metal-poor Clouds than in the Galaxy, in agreement with theoretical expectations (e.g. Becker & Iben 1980).

Meatheringham & Dopita (1991) obtained optical spectra of 73 LMC and SMC PNe and Dopita & Meatheringham (1991) applied a grid of photoionization models to these observations to derive nebular abundances and central star effective temperatures, luminosities and masses (Fig. 8).

4.1 The HST Era

The first spatially resolved images of Magellanic Cloud PNe were published by Blades et al. (1992), who presented pre-COSTAR Faint Object Camera [O III] 5007 Å images of two SMC PNe and one LMC PN, with 50 milli-arcsec resolution (the FOC was the only instrument that reached the HST's optical diffraction-limited resolution). One LMC nebula N 66 (=WS 35), was found by them to have a particularly unusual morphology, showing multiple lobes and a bright central star.

In a series of papers, Dopita, Vassiliadis and collaborators have published WFPC and WFPC-2 [O III] images of Magellanic Cloud PNe obtained over several HST cycles, mostly pre-COSTAR, while Stanghellini et al. (1999) have

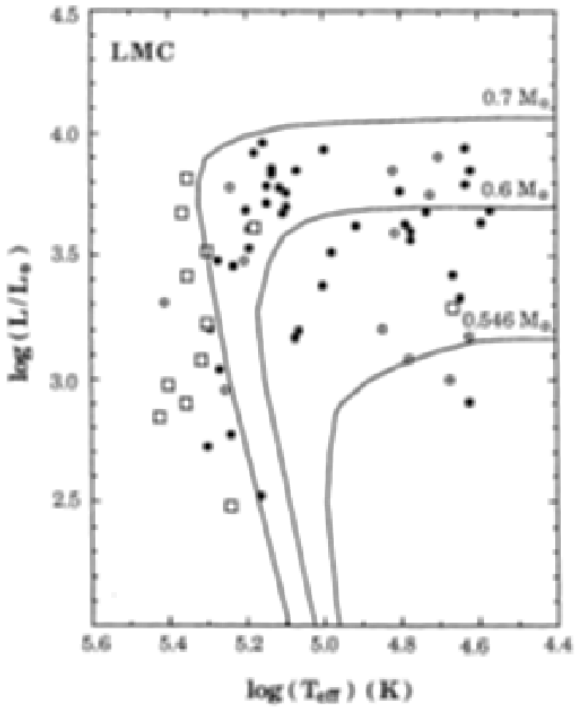

Fig. 8. Hertzsprung-Russell diagram for LMC PN central stars, together with H-burning evolutionary tracks for three different core masses. From Dopita & Meatheringham (1991).

published pre-COSTAR (and some post-COSTAR) HST FOC images of 27 Magellanic Cloud PNe taken in the [O III] line, some examples of which are shown in Fig. 9.

Vassiliadis et al. (1996) presented HST FOS UV spectra for a number of Magellanic Cloud PNe, while Dopita et al. (1997) have fitted photoionization models to the combined UV+optical spectra of 10 of these PNe in the LMC. Central star effective temperatures and luminosities were derived, with a star being classed as an H-burner or a He-burner according to which evolutionary track gave an age in agreement with the nebular expansion age (given by the measured nebular radius and expansion velocity). Fig. 10 shows one of their spectral fits, as well as the HR diagram for the objects assigned as He-burners.

The addition of STIS to its instrument suite powerfully increased the HST's capabilities for studies of Magellanic Cloud PNe, with STIS's ability to obtain slitless spectral imaging in multiple emission lines making a particularly strong impact. Shaw et al. (2001) have presented STIS images for 29 LMC PNe, obtained as part of an HST Snapshot survey. The overall sample of 60 LMC PNe which had HST images showed a much higher incidence of non-symmetric neb-

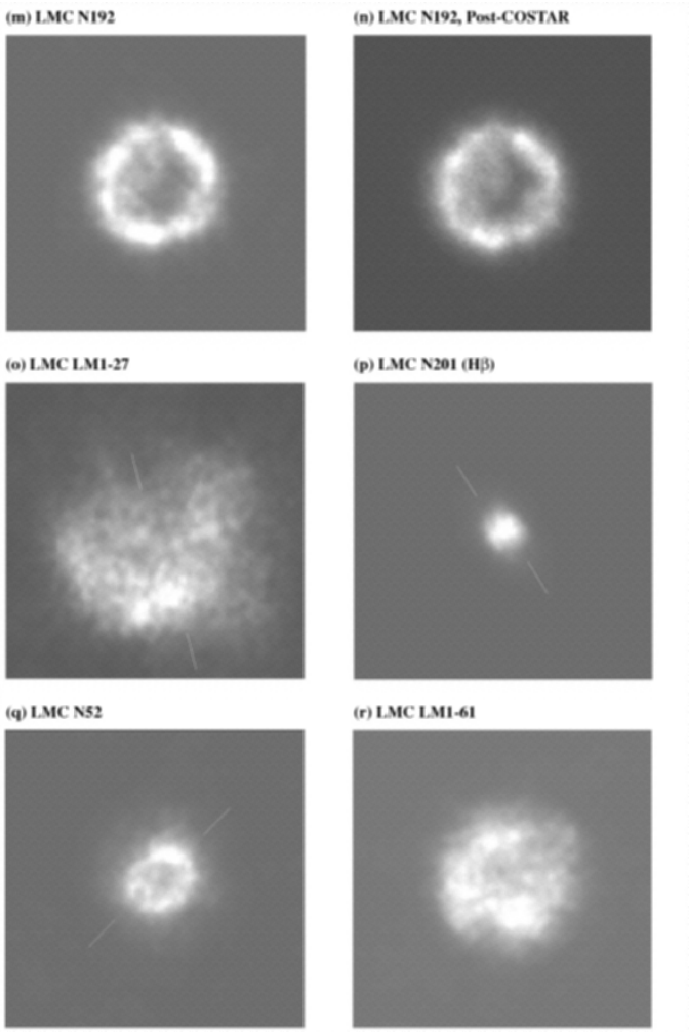

Fig. 9. HST Faint Object Camera images of five LMC PNe taken in the [O III] 5007 Å line. Each image is 2.2 arcsec on a side. From Stanghellini et al. (1999).

ulae than do comparable Galactic PN samples. Stanghellini et al. (2002) have presented STIS slitless spectra of 29 more LMC PNe (some examples are shown in Fig. 11), while Stanghellini et al. (2003) presented STIS images and slitless spectra for 27 more SMC PNe.

Pĕna et al. (1994) discovered that the central star of LMC N66 was much brighter at IUE UV wavelengths in the 1990's than it was in the 1980's. Since then, it has been monitored closely. It reached maximum brightness in 1994 and by 2000 had faded to a fainter level than in 1983. Since 1994 its optical and UV

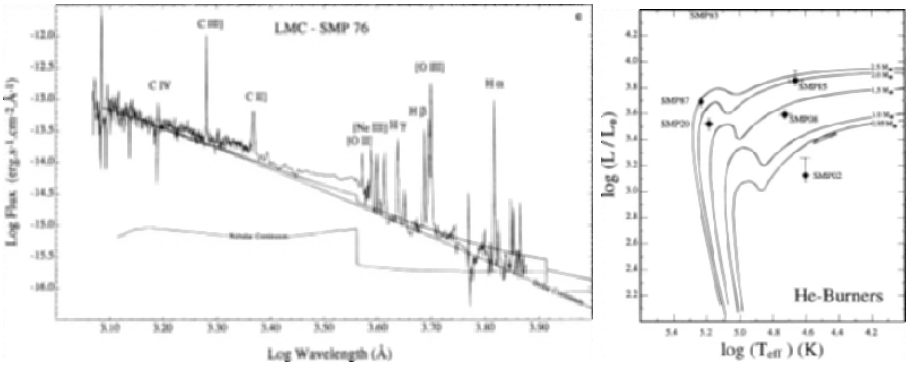

Fig. 10. Left: model stellar + nebular continuum fit to the UV+optical energy distribution of LMC SMP 76. Right: Hertzsprung-Russell diagram showing central star locations, together with He-burning stellar evolutionary tracks that are labelled by their initial main sequence masses. From Dopita et al. (1997).

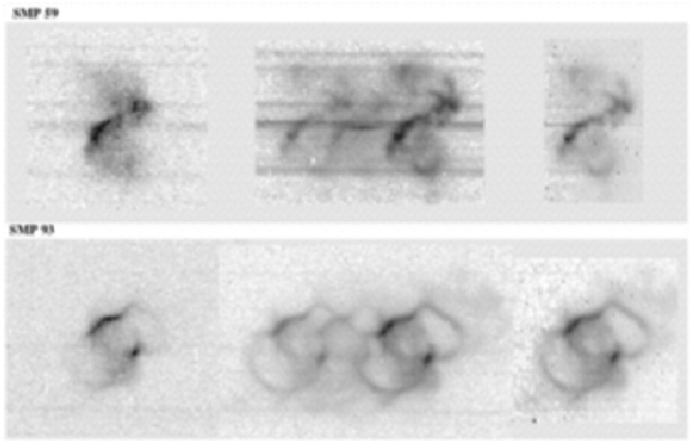

Fig. 11. HST STIS slitless spectra of the LMC PNe SMP 59 (LM 2-25) and SMP 93 (N 181). The images on the left are in the [O III] 5007 Å line, those in the middle show the Hα plus [N II] 6548, 6584 Å blend, and those on the right are deblended [N II] images. From Stanghellini et al. (2002).

spectrum has been that of a WN star, the only known case amongst PN nuclei. Fig. 12 shows an HST FOC [O III] image of LMC N66, from Pẽna et al. (2004), while Fig. 13 shows a sequence of IUE and HST UV spectra, from Hamann et al. (2003), which nicely illustrates the rise and fall of the central star's brightness. Hamann et al. suggested that rather than this being a final thermal pulse event, its nucleus may be a white dwarf accreting matter from a companion and could be the precursor to a Type Ia supernova.

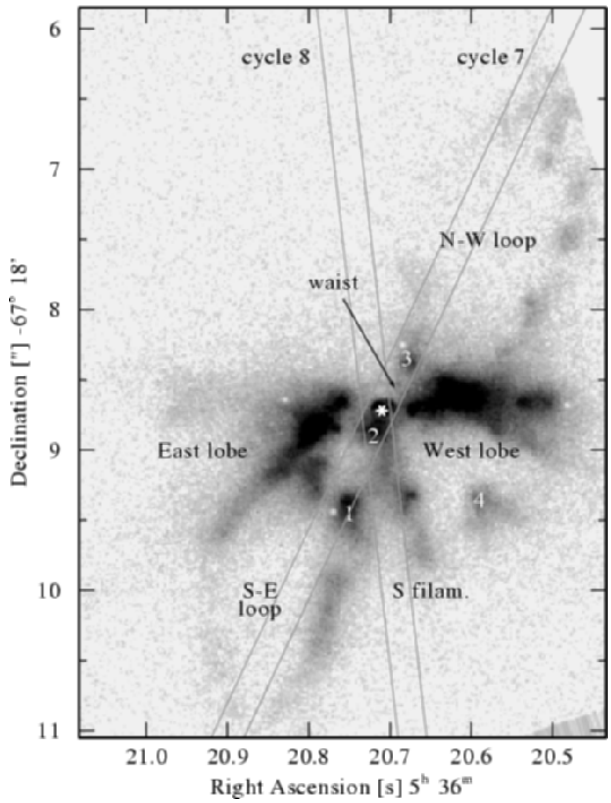

Fig. 12. HST Faint Object Camera (not WFPC) image of LMC N66 (=WS35) in the [O III] 5007 Å line, acquired in February 1994 when the central star was near peak brightness. From Pĕna et al. (2004).

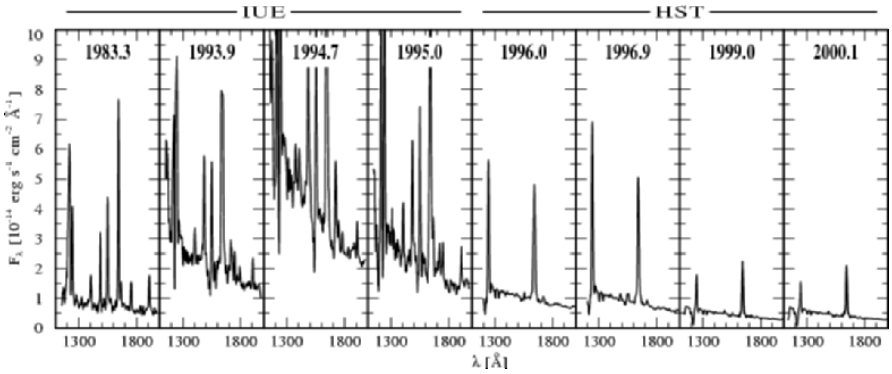

Fig. 13. A time sequence of 1200-2000 Å IUE and HST spectra of the central star of LMC N66, showing the transient brightening event that peaked in 1993-4. From Hamann et al. (2003).

References

1. M. Arnaboldi et al.: ApJ, **472**, 145 (1996)
2. M. Arnaboldi et al.: ApJ, **507**, 759 (1998)
3. S. A. Becker, I. Iben Jr.: ApJ, **237**, 129 (1980)
4. J. C. Blades et al.: ApJ, **398**, L41 (1992)
5. R. Ciardullo et al.: ApJ, **339**, 53 (1989a)
6. R. Ciardullo, G. H. Jacoby, H. C. Ford: ApJ, **344**, 715 (1989b)
7. M. A. Dopita et al.: ApJ, **327**, 639 (1988)
8. M. A. Dopita, S. J. Meatheringham: ApJ, **377**, 480 (1991)
9. M. A. Dopita et al.: ApJ, **474**, 188 (1997)
10. J. J. Feldmeier, R. Ciardullo, G. H. Jacoby: ApJ, **503**, 109 (1998)
11. H. C. Ford, D. C. Jenner, H. W. Epps: ApJ, **183**, L73 (1973)
12. H. C. Ford, D. C. Jenner: ApJ, **202**, 365 (1975)
13. W. -R. Hamann et al.: A&A, **409**, 969 (2003)
14. K. G. Henize: ApJS, **2**, 315 (1956)
15. G. H. Jacoby: ApJS, **42**, 1 (1980)
16. E. M. Lindsay: AJ, **66**, 169 (1961)
17. E. M. Lindsay, D. J. Mullan: Irish AJ, **6**, 51 (1963)
18. L. Magrini et al.: A&A, **407**, 51 (2003)
19. S. J. Meatheringham et al.: ApJ, **327**, 651 (1988)
20. S. J. Meatheringham, M. A. Dopita: ApJS, **75**, 407 (1991)
21. R. H. Méndez et al.: ApJ, **491**, L23 (1997)
22. R. H. Méndez, T. Soffner: A&A, **321**, 898 (1997)
23. R. H. Méndez et al.: ApJ, **563**, 135 (2001)
24. D. J. Monk, M. J. Barlow, R. E. S. Clegg, MNRAS, **234**, 583 (1988)
25. M. Pēna et al.: ApJ, **428**, L9 (1994)
26. M. Pēna et al.: A&A, **419**, 583 (2004)
27. N. Sanduleak, D. J. MacConnell, A. G. D. Philip: PASP. **90**, 621 (1978)
28. R. A. Shaw et al.: ApJ, **548**, 727 (2001)
29. L. Stanghellini et al.: ApJ, **510**, 687 (1999)
30. L. Stanghellini et al.: ApJ, **575**, 178 (2002)
31. L. Stanghellini et al.: ApJ, **596**, 997 (2003)
32. T. Theuns, S. J. Warren: MNRAS, **284**, L11 (1997)
33. E. Vassiliadis et al.: ApJS, **105**, 375 (1996)